Production and Implementation of GPS Auxiliary Observations for Satellite Navigation Positioning

C. C. Chang* and P. Y. Cheng

Department of Applied Geomatics, Chien Hsin University of Science and Technology

ABSTRACT

Using satellites for positioning is difficult in urban areas because buildings obstruct the signals of GPS. Such obstruction can reduce positioning precision or even disable positioning. Without using additional auxiliary systems, two prior epochs from single point positioning (SPP) results were used to calculate the initial coordinates of an unknown point, and then the orbital positions of obstructed satellites were used to perform inverse computations to calculate a geometric range. Subsequently, the previous two epochs of observations were inverted to obtain the pseudo-range errors; from that, the so-called virtual range (VR) was calculated at the epoch of positioning. In this study, static data was first used for SPP tests. The results showed that regardless of how many VR results were incorporated, the horizontal positioning error was smaller than 0.2 m. However, when the vertical precision was considered, incorporating only a small number of VRs, one or two, just ensured the reliability of the result (i.e., error smaller than 2DRMS). Moreover, the results of navigation positioning tests on kinematic data revealed that when observations were only taken from three satellites, introducing one auxiliary VR observation was sufficient to obtain the positioning solution. However, this approach was only reliable in the plane coordinates. As for VR observations in the kinematic mode, the simulated beacon range (BR) was incorporated for resection positioning. It was discovered that using observations composed of both VRs and BRs resulted in reliable positioning in both vertical and horizontal components, proving that low elevation wireless beacon in obstructed environments was applicable to assist satellite navigation positioning.

Keywords: obstructed satellite, near-ground beacon, auxiliary observation, satellite navigation positioning

GPS 導航定位輔助觀測量之產製與運用

張嘉強* 鄭佩宇

健行科技大學應用空間資訊系

摘 要

在衛星定位屬於艱困環境中的都會區內，建物會遮蔽 GPS 衛星訊號，導致定位精度降低，甚至無法定位。在不增加輔助系統下，本研究嘗試利用先前二筆單點定位(SPP)成果，先推算出待定位點之初始坐標，再配合遮蔽衛星之軌道位置，反算出一組幾何距離，另把先前二筆觀測量反演取得之虛擬距離誤差加入，即可得出定位時刻之所謂「虛假距離(VR)」。本研究先

文稿收件日期 107.12.25;文稿修正後接受日期 108.10.25; *通訊作者
Manuscript received December 25, 2018; revised October 25, 2019; * Corresponding author

利用靜態資料進行單點定位測試，成果顯示在引入不同數量之 VR 後，平面定位誤差與真實觀測量 SPP 成果之差異量級可小於 0.2 m，但若兼顧垂直分量精度，則引入 1-2 個之少量 VR，方可確保成果之可靠性(即定位誤差小於2DRMS)。另針對動態資料之導航定位測試成果可知，在觀測數量只有 3 顆衛星時，藉由 1 個 VR 觀測量的引入即可獲得定位解，但也只有在平面坐標上較具可靠性。另針對動態模式之 VR 觀測量，輔以近地信標之模擬感測距離(BR)，採空間交會定位進行解算之成果可知，VR 與 BR 之組合觀測量多可在平面及垂直分量上同時取得可靠之定位成果，可見低角度無線信標在透空遮蔽環境下之運作，或可對衛星導航之輔助定位具有一定程度之應用價值。

關鍵詞：遮蔽衛星、近地信標、輔助觀測量、衛星導航定位

Ⅰ. INTRODUCTION

Conventional navigation systems on automobiles using satellite positioning technology and electronic maps have become part of our mobile lives. As automobile technology advances, self-driving cars have become almost practical for real-world applications; passengers only need to set the desired destination and the self-driving car would take them to the destination. When driving on a road, a self-driving car can exchange information with cars around it, thereby maintaining the safe distance even driving with a high speed. With self-driving cars, accidents due to human factors would be possibly avoided, and the roads would be able to accommodate more traffic.

To achieve completely autonomous driving, various related technologies in four major categories, namely positioning, imaging, radar detection and control system, have been developed. Sensors required in those technologies include Global Positioning System (GPS)/Global Navigation Satellite System (GNSS) receivers, laser rangefinders, laser scanners, cameras, radars, odometers and controllers. The most common positioning system, comprising GPS/GNSS, odometer and electronic map, such as Google Maps, can conduct comprehensive location detection. The functions of this system are to obtain the current location of a self-driving car, to record the paths it takes and to plan optimal paths to avoid congested roads and to minimize driving time.

GPS/GNSS is a positioning system centered on satellites. Its basic theory is to use the signals received at an unknown point from at least four satellites to conduct three-dimensional positioning. The primary weakness in the operation of this system is that satellite signal transmission may be obstructed by obstacles, resulting in blockage of the direct signal between the satellite and receiver, consequently limiting positioning effectiveness and causing errors. In such situations, additional auxiliary technologies for safety are required [1].

Among all satellite positioning environments, urban areas are considered challenging because of their dense buildings and structures that obstruct GPS/GNSS signals. When satellite signal directions across streets are obstructed, only satellite signals transmitted along the streets can be received [2]. Subsequently, the geometric constellation of the satellites and the quality of signals may substantially reduce the positioning precision by an average of 25 m or even by over 100 m [3]. In extreme situations when the ratio of building height and street width is high, an insufficient number of satellite signals may be received, resulting in the failure to conduct positioning at all.

In high-precision mobile mapping, a system integrating an inertial navigation system (INS) and a GPS/GNSS can constitute a seamless observation system for position, speed and orientation [4]. However, due to the high expense of high-quality INS, their application in navigation is still uncommon. For those GNSS-related positioning systems, pseudo-satellite (known as pseudolite) can use GNSS signal generators to provide near-ground line-of-sight ranges required for positioning, but its high costs also trap it in the promotion stage [5].

Advances in communication technology have developed out of the need for mobile positioning based on assisted-GNSS (A-GNSS).

Devices can provide positions with the assistance of information transmitted through wireless networks in GNSS signals denial environments [6]. However, in practice, this technology still requires intensive support from WiFi and Cell-ID to provide positioning services. This reliance imposes an extra burden in providing assistance information for navigational positioning [7].

To overcome the needs for mobile positioning in areas where is difficult to receive GNSS signals, the positioning technologies, such as WiFi, ultrawideband (UWB), signal of opportunity (SOP), laser, dead reckoning, map matching and GNSS shadow matching etc., have been developed and have the potential for real-life application [8][9][10]. However, any relatively straightforward technology using easy-obtained auxiliary information for GNSS navigation positioning still needs to be explored to ensure the availability of GNSS navigation positioning.

Therefore, a novel method of producing auxiliary data, along with positioning algorithm and application modes, was proposed and discussed by this study. It was aimed at using simple and low-cost computations to achieve navigation positioning under challenging GNSS signal obstruction or jamming conditions.

Based on the aforementioned purpose, this study focused on GPS navigation positioning with the help of obstructed satellite signals. The geometric distances between the satellites and the anchor points were reorganized to construct auxiliary observations under difficult satellite conditions. GPS navigation positioning was tested using these auxiliary observations to investigate the performances of the positioning results. Moreover, to consider the potential of using near-ground wireless beacons, simulated beacon ranges (BRs) were incorporated into the auxiliary observations, for which spatial resections were calculated to evaluate the applicability and precision of the proposed navigation positioning.

Ⅱ. POSITIONING METHOD OF USING AUXILIARY OBSERVATION

This study focused on the investigation of the acquisition and application of auxiliary observation for satellite navigation. The main concern was the influence of GNSS satellite signal blockage in urban areas. If the so-called virtual ranges (VRs) between the obstructed satellites and the receivers could be reconstructed or if near-ground sensed beacon ranges (BRs) could be incorporated for positioning, then the applicability of satellite navigation based on the mode of single point positioning (SPP) could be increased. The concept is illustrated in Fig. 1.

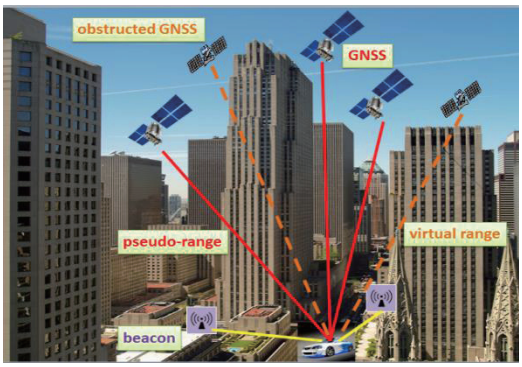

Fig. 1 Obtaining auxiliary data in urban areas for positioning

2.1 Producing VR of an Obstructed Satellite

The concept of using signals of obstructed satellite to obtain auxiliary data when the satellite observations are insufficient has been successfully utilized in reproducing observations for pseudolites and has been applied to the development of using single WiFi access point (AP) to conduct indoor positioning [11][12].

To reconstruct the geometric range for an obstructed GNSS satellite, a sufficient number of GNSS satellite observations must be obtained in advance for at least two epochs. Based on this premise, the SPP solutions at these two epochs (t_1 and t_2) are converted to plane coordinates and height (E, N, h), referred to TM2° local system and geometric height, followed by using dead reckoning (DR) algorithm to calculate subsequent approximate coordinates (E_i, N_i, h_i) for the location to be determined at epoch t_i. The calculation process can be expressed as follows:

$$\alpha_{12} = \tan^{-1}\frac{E_2 - E_1}{N_2 - N_1} \quad (1)$$

$$V_{12} = \frac{S_{12}}{\Delta t} = \frac{\sqrt{(E_2 - E_1)^2 + (N_2 - N_1)^2}}{t_2 - t_1} \quad (2)$$

$$S_{2i} = V_{12} \times (t_i - t_2) \quad (3)$$

$$E_i = E_2 + S_{2i} \sin \propto_{12} \quad (4)$$

$$N_i = N_2 + S_{2i} \cos \propto_{12} \quad (5)$$

$$h_i = h_2 + \frac{(h_2 - h_1)}{\Delta t} \quad (6)$$

where α, V and S are the moving azimuth, velocity and distance, respectively, between the two successive epochs.

After obtaining the approximate coordinates of the location at t_i, an appropriate number of obstructed satellites were selected. Based on the previously downloaded IGS ultra-rapid ephemeris, two epochs of satellite positions, 15 minutes prior to and after t_i, were adopted. Linear interpolation was then used to determine the 3-D coordinates of the selected satellite (X^{os}, Y^{os}, Z^{os}) at the epoch of t_i.

The approximate coordinates (E_i, N_i, h_i) obtained in Eq. (1-6) were converted to the 3-D geocentric coordinate (X_i^0, Y_i^0, Z_i^0). Subsequently, the pseudo-range error (ε_i^{os}) of the obstructed satellite at the epoch of t_i was incorporated to obtain the reconstructed virtual range between the unknown point and the obstructed satellite. This reconstructed range was similar to a real pseudo-range (PR) observable; it was denoted as virtual range (VR), and was calculated as follows:

$$VR_i = \sqrt{(X_i^{os} - X_i^0)^2 + (Y_i^{os} - Y_i^0)^2 + (Z_i^{os} - Z_i^0)^2} + \varepsilon_i^{os} \quad (7)$$

To calculate the PR error (ε_i^{os}), the geometric ranges (R^{os}) at t_1 and t_2 must be obtained using the corresponding SPP solutions and the satellite positions. In addition, the pseudo-ranges of the obstructed satellite (PR^{os}) received at t_1 and t_2 were taken out from the observation file. The two epochs of ε_1^{os} and ε_2^{os} were then determined by Eq. (8). Finally, the pseudo-range error (ε_i^{os}) at the epoch of t_i for each obstructed satellite is expressed in Eq. (9).

$$\varepsilon_2^{os} = PR_2^{os} - R_2^{os} \; ; \quad \varepsilon_1^{os} = PR_1^{os} - R_1^{os} \quad (8)$$

$$\varepsilon_i^{os} = \left(\frac{\varepsilon_2^{os} - \varepsilon_1^{os}}{\Delta t}\right) \times (t_i - t_2) \quad (9)$$

Based on the aforementioned method, there are two restrictions on applying the VR observation:

(1) The approximate coordinate of the unknown point at t_i was obtained by dead reckoning using the previous two epochs of positioned coordinates, in which the mathematical model was based on a linear moving condition. Therefore, the VR constructed by this study can be applied to either static mode of SPP or kinematic mode of objects that move only at steady speeds along linear paths.

(2) To obtain ε_i^{os} for obstructed satellites, positioned coordinates from the two previous epochs were first used to invert their pseudo-range errors, along with the satellite orbits, and then a linear interpolation was conducted to obtain the predicted error at t_i. Because ε_i^{os} is influenced by complex factors such as clock error, ionospheric error and tropospheric error, it can change substantially with time. Therefore, the use of VR for data reconstruction must be restricted to points within a limited time interval (such as within 3–5 seconds).

2.2 Simulating BR of an Near-ground Beacon

As the implementation of wireless beacons broadens, scholars have become interested in using beacons to provide auxiliary data for positioning. The signals transmitted by beacons and received at unknown points to obtain the sensing range of BR was used, with which the coordinates of the beacons pre-stored were integrated, as auxiliary data for position computation.

This study incorporated near-ground BRs and employed resection models to test positioning. Although large-scale outdoor beacons ranging to a working distance of 120 m existed on the market for transportation purposes, they were difficult to real test in experiments, due to their high cost and communication frequencies. Therefore, this study used simulation to obtain BR for assisted positioning. The simulation algorithm can be expressed as

follows:

$$BR_i = \sqrt{(X^B - X_i^0)^2 + (Y^B - Y_i^0)^2 + (Z^B - Z_i^0)^2} + \varepsilon_i^B \quad (10)$$

where (X^B, Y^B, Z^B) are the spatial coordinates of a near-ground beacon. It is assumed that beacons were constructed 3 m above ground. (X_i^0, Y_i^0, Z_i^0) are the approximate coordinates at t_i and are obtained using Eq. (1-6). ε_i^B is the sensing error of the BR, set to be a random error within ±0.2 m.

2.3 Calculating Position Using Different Combinations of Ranges

Regarding the signal blockage problem faced by satellite positioning in urban areas, if an appropriate number of obstructed satellites can be adopted to reconstruct the VRs, mainly based on the spatial distance obtained through inverse computation with the approximate coordinate of the unknown point and the satellite coordinate, this auxiliary observations can be applied to assist navigation positioning.

In implementation, the reconstructed VR is similar to the real PR, so using either only VRs or both VRs and PRs are possible to carry on positioning for satellite navigation. The operation is depicted in Fig. 2. In this study, the conventional SPP was conducted using the open source package RTKLIB for position computation [13].

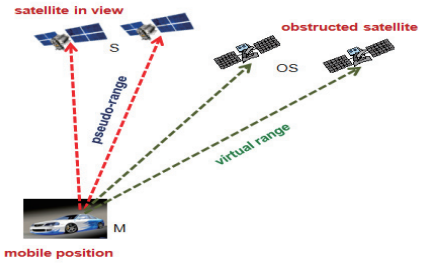

Fig. 2 Operational model using VR to assist in positioning

In data processing, as the simulated BR did not contain GNSS-related observation error, the characteristics of BR differed from those of the actual PR. Consequently, BR and PR could not be directly combined in SPP computation.

When conducting this positioning calculation, the observations of PR or VR were not actually adopted. Instead, the pure geometric range of GRs calculated using the approximate coordinates of the unknown point and the satellite positions in orbit (X^s, Y^s, Z^s) were utilized. The GRs together with BRs were combined to provide sufficient range observations for positioning. The operation is illustrated in Fig. 3.

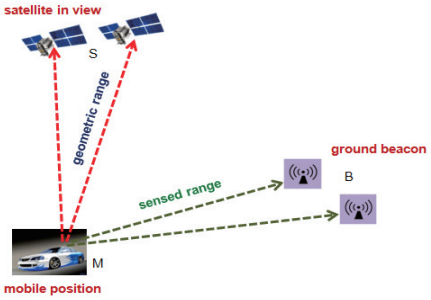

Fig. 3 Operational model using BR to assist in positioning

The positioning calculation using this set of combined data was based on the spatial resection model. When a case of using two GRs and two BRs is taken as an example, the residual equation (V=AX−L) can be expressed as follows:

$$\begin{bmatrix} V_M^{S1} \\ V_M^{S2} \\ V_M^{B1} \\ V_M^{B2} \end{bmatrix} = \begin{bmatrix} -\left(\frac{X^{S1}-X_0}{GR_0^{S1}}\right) & -\left(\frac{Y^{S1}-Y_0}{GR_0^{S1}}\right) & -\left(\frac{Z^{S1}-Z_0}{GR_0^{S1}}\right) \\ -\left(\frac{X^{S2}-X_0}{GR_0^{S2}}\right) & -\left(\frac{Y^{S2}-Y_0}{GR_0^{S2}}\right) & -\left(\frac{Z^{S2}-Z_0}{GR_0^{S2}}\right) \\ -\left(\frac{X^{B1}-X_0}{BR_0^{B1}}\right) & -\left(\frac{Y^{B1}-Y_0}{BR_0^{B1}}\right) & -\left(\frac{Z^{B1}-Z_0}{BR_0^{B1}}\right) \\ -\left(\frac{X^{B2}-X_0}{BR_0^{B2}}\right) & -\left(\frac{Y^{B2}-Y_0}{BR_0^{B2}}\right) & -\left(\frac{Z^{B2}-Z_0}{BR_0^{B2}}\right) \end{bmatrix} \begin{bmatrix} \Delta X_M \\ \Delta Y_M \\ \Delta Z_M \end{bmatrix} - \begin{bmatrix} GR_M^{S1} - GR_0^{S1} \\ GR_M^{S2} - GR_0^{S2} \\ BR_M^{B1} - BR_0^{B1} \\ BR_M^{B2} - BR_0^{B2} \end{bmatrix} \quad (11)$$

By using observations of GRs and BRs as well as the approximate coordinates of the unknown point (X_0, Y_0, Z_0), the equation of $X=(A^TA)^{-1}A^TL$ can be solved for the increment of the unknown $(\Delta X_M, \Delta Y_M, \Delta Z_M)$ through

iteration; and the three-dimensional coordinates of the unknown point ($X=[X_M, Y_M, Z_M]^T$) can be obtained.

III. TESTING RESULTS AND ANALYSIS

Two operational models regarding the use of auxiliary data of VR and BR for satellite navigation positioning were proposed. As this study focused primarily on data generation method, the real-time data processing was not essential. As a result, the solutions evaluated for the applicability of auxiliary data were all obtained by post-processing.

The data testing processes in this study were separated into two types, namely static data and kinematic data. The static testing data were collected on the university campus; the kinematic testing data were obtained from a car driving at an average speed of 65 km/hr on the Highway 66 nearby Zhongli district.

Regarding the acquisition and application of GNSS data, the observations were received using a NovAtel DL-V3 receiver. The data interval was set to be 1 Hz. To simplify the tests, the VRs used for processing were only made for GPS L1 code range. To simulate an obstructed situation, the satellite observations were adopted from only four to five satellites with the highest elevation angles. During the positioning computation, the satellite positions were taken from the real-time mode of broadcast ephemeris.

It has been noted that the approximate coordinates of unknown points were obtained using data from two previous epochs that had sufficient satellite observations for successful SSP. The auxiliary observations were formed and tested for the subsequent three epochs of data, based on the scenarios of satellites obstructed partially or totally. To evaluate the precision of positioning results, the coordinate solutions of three epochs of data that used auxiliary observations were compared with the known coordinates that were pre-surveyed by static or kinematic mode with a centimeter-level precision. The root mean square errors (RMSEs) of the overall test data set were finally provided.

To determine if the results were applicable, the distance root mean squared (DRMS) of the SPP solutions served as the basis, and 2DRMSE, representing 95% probability, was selected to judge if the positioning results using auxiliary data met the safety standard or not [14]. The horizontal and vertical components of the coordinate solutions were expressed separately.

3.1 VR-assisted Static SPP

In this test, the testing point did not move. The VR observations generated for obstructed satellites were combined with original PR observations of the satellites to perform static SPP using different number combinations. The testing results are listed in Tab. 1, where SPP represents the positioning results of all satellites using only the real PR observations, 2D indicates the horizontal component of the coordinates and U represents the vertical component.

Tab. 1 VR-assisted static SPP testing results

Mode	RMSE (m)	
	2D	U
5PR (SPP)	1.83	1.07
4PR+1VR	1.88	0.99
3PR+2VR	2.00	0.87
2PR+3VR	1.96	2.47
1PR+4VR	1.73	2.80
0PR+5VR	1.61	2.04

Referencing the positioning errors in Tab. 1, a comparison of the errors in horizontal component for each observation combination is depicted in Fig. 4, whereas a comparison of vertical errors is presented in Fig. 5. In each figure, the purple dashed line is the reference line that stands for the SPP error, whereas the red dashed line is the 2DRMS. For this test, the 2DRMS of the horizontal component was 3.66 m, and the vertical component was 2.14 m.

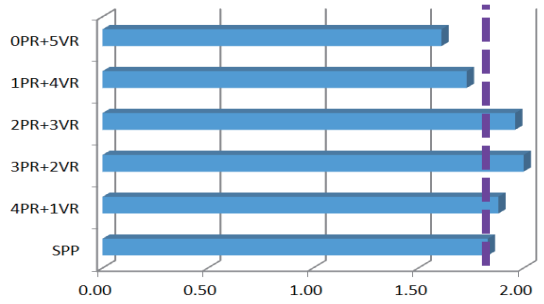

Fig. 4 Comparing horizontal errors of VR-assisted static SSP results (unit: m)

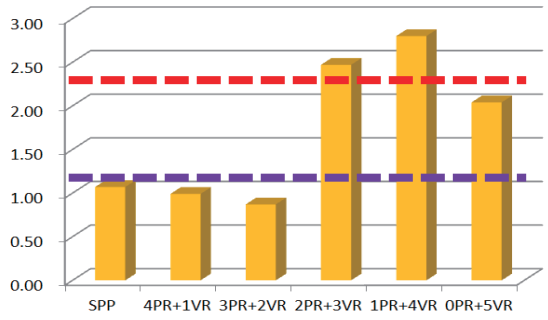

Fig. 5 Comparing vertical errors of VR-assisted static SSP results (unit: m)

The results revealed that in all combinations of using different numbers of VR observations for static SPP, when compared against the real PR-based SPP errors, the horizontal errors were no one greater than 2DRMS of the safety standard, and the differences between them and the horizontal errors of SPP were all smaller than 0.2 m. By contrast, for vertical components, when more VR observations were introduced, errors larger than 2DRMS easily appeared. Therefore, when considering both horizontal and vertical positioning errors, introducing one to two VR observations in obstructed environments is a more reliable strategy.

For those solutions by introducing VRs and performing better than SPP using PRs, they may relate to the observations supplemented with the enhancement of satellite geometry. However, this explanation is still required for a further proof (the same remarks are also given to the following sections of tests and analysis).

3.2 VR-assisted Kinematic SPP

This section details the testing data in which the points moved. The kinematic testing results using combinations of different numbers of VR observations and original PR observations are listed in Tab. 2.

Tab. 2 VR-assisted kinematic SPP testing results

Mode	RMSE (m)	
	2D	U
4PR (SPP)	6.60	8.36
3PR+1VR	4.35	71.33
2PR+2VR	16.16	100.50
1PR+3VR	17.76	107.80
0PR+4VR	22.54	3.03

Referencing the positioning errors in Tab. 2, a comparison of the errors in horizontal component for each observation combination is depicted in Fig. 6, whereas a comparison for errors of vertical component is presented in Fig. 7. Under this test, the safety positioning reference lines represented the 2DRMS were at 13.20 m and 16.72 m for horizontal and vertical component, respectively.

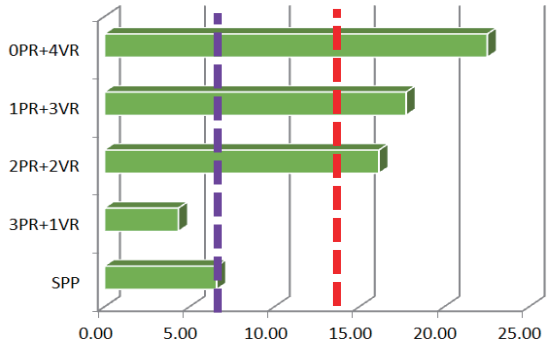

Fig. 6 Comparing horizontal errors of VR-assisted kinematic SPP results (unit: m)

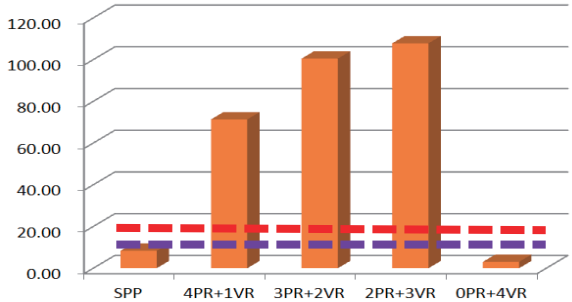

Fig. 7 Comparing vertical errors of VR-assisted kinematic SPP results (unit: m)

The results of this test, conducting kinematic SPP using different numbers of VR observations, were only safe in the horizontal component when introducing one VR observation. However, the solution using one VR observation showed that the vertical error substantially exceeded 2DRMS of the safety standard. If only VR observations were used, the vertical error met the safety standard, and the magnitude of error was even superior to that of the SPP results.

A comprehensive consideration revealed that when the satellite number received was less than four, introducing one VR observation might provide the navigation solutions, although only its horizontal coordinates were safe. Whether using only VR observations can optimize the vertical coordinates for kinematic SPP, it requires further testing with more data.

3.3 BR-assisted Kinematic Resection Positioning

Also under the condition of the moving points, this section of tests combined the simulation ranges of BR with different numbers of VR observations to conduct positioning through a spatial resection algorithm. When conducting near-ground BR simulation, as the satellites in view were mostly located within the azimuth of 0°-180°, two beacons were simulated to be set up at azimuth of 180°-270° and 270°-360°. The testing results are shown in Tab. 3.

Tab. 3 BR-assisted kinematic resection testing results

Mode	RMSE (m)	
	2D	U
4PR(SPP)	6.60	8.36
3VR+1BR	7.01	7.24
2VR+2BR	6.46	7.38
3VR+2BR	6.42	7.41

Referencing the positioning errors in Tab. 3, comparisons of different combinations are graphed in Fig. 8 and Fig. 9 for horizontal and vertical errors, respectively. Because the satellite observations used in this test were identical to those in Tab. 2, the reference lines marking safe standard also represented the same 2DRMS values.

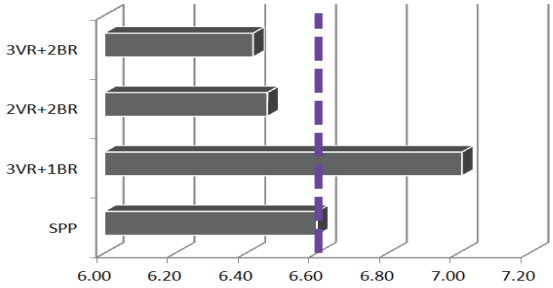

Fig. 8 Comparing horizontal errors of BR-assisted kinematic resection results (unit: m)

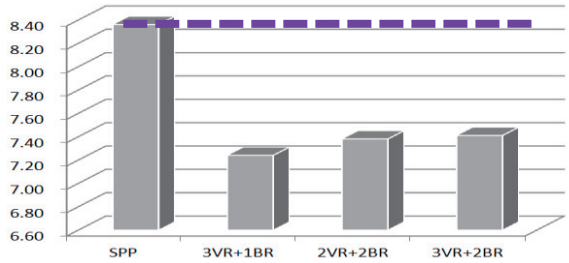

Fig. 9 Comparing vertical errors of BR-assisted kinematic resection results (unit: m)

The results of this test revealed that under the kinematic mode, using a small number of near-ground BRs to conduct resection positioning, together with VR observations, achieved positioning errors of the same level as using SPP. In addition, when using a small number of VR and BR observations, different combinations all led to a stable performance, i.e. differences smaller than 0.6 m, for both horizontal and vertical components. Therefore, it is expected that if the real sensed BR errors did not differ greatly from the simulation quantities, i.e. ± 0.2 m, the proposed beacon assisted positioning method would be applicable.

IV. CONCLUSIONS AND SUGGESTIONS

In urban areas, GNSS satellite signals are often obstructed so that the applicability of navigation positioning is reduced. This study tried to reconstruct the obstructed satellite's

range observations (VRs) and to introduce the near-ground beacon ranges (BRs) as the auxiliary data to assist navigation positioning.

The testing results showed that regardless of whether the unknown points are static or kinematic, reconstructed VRs could achieve applicable positioning results, if a small number of VRs are adopted. However, the positioned horizontal coordinates are of more reliability. In addition, in the kinematic mode, using a small number of BRs to conduct spatial resection yields three-dimensional coordinates within a certain safety level, making them suitable for practical applications.

The auxiliary observations produced by this study have tested and realized several applicable conditions. However, the testing samples are still not enough and await future expansion. Still, the relevant directions for technical improvement have been established by this study. For example, the following topics are all worthy of expansion and investigation:

(1) How sensors can be introduced to improve the precision of the approximate coordinate at an unknown point?

(2) Whether using any sensors or electronic maps can effectively determine the location of an unknown point after a vehicle making a turn?

(3) Whether any rule is required to select the obstructed satellites based on their better geometric allocation?

(4) How an optimized PR error model can be constructed and implemented, in particular to enhance the reliability of vertical solutions?

(5) What are the geometric effects of setting up the near-ground beacons?

(6) What are the characteristics of using pure VR or BR observations in position computations?

(7) How to integrate various types of observations, such as PRs, VRs and BRs, into a positioning algorithm with a weighting function?

ACKNOWLEDGEMENTS

The authors are grateful to the Ministry of Science and Technology for funding this project under the contract number of MOST 106-2119-M-231-001.

REFERENCES

[1] Auld, J., “A Focus on Safety”, Velocity, NovAtel Inc., pp. 6-11, 2016.

[2] Groves, P. D. and Ziebart, M. K., “Shadow Matching: Improved GNSS Accuracy in Urban Canyons”, GPS World, Feb issue, 2012.

[3] Groves, P. D., “It’s Time for 3D Mapping-Aided GNSS”, Inside GNSS, Sep/Oct issue, pp. 50-56, 2016.

[4] Chiang, K. W., Duong, T. T. and Liao, J. K., “The Performance Analysis of a Real-Time Integrated INS/GPS Vehicle Navigation System with Abnormal GPS Measurement Elimination, Sensors”, Vol. 13, No. 8, pp. 10599-10622, 2013.

[5] GPS World, “Syntony Rises High by Going Underground”, Nov issue, pp. 35, 2016.

[6] Monnerat, M., “AGNSS Standardization: The Path to Success in Location-based Services”, Inside GNSS, Vol. 3, No. 5, pp. 23-33, 2008.

[7] Murfin, T., “Rx Networks: Commercializing Indoor Location”, GPS World, Nov issue, 2014.

[8] Groves, P. D., “Four Key Challenges to Multi-sensor PNT”, IEEE/ION Position Location and Navigation Symposium (PLANS), Monterey, California, 2014.

[9] GPS World, “Opportunity for Accuracy: Exploiting Terrestrial Signals of Opportunity”, March issue, pp. 23-29, 2016.

[10] GPS World, “Terrestrial Beacons Bring Wide-Area Location Indoors”, July issue, pp. 38-40, 2016.

[11] Chang, C. C., Lou, P. C. and Ke, P. J., “Test of Simulated Pseudolite Measurement Applied to GPS and Multi-Pseudolite Integrated Positioning”, Survey Review, Vol. 40, No. 309, pp. 212-220, 2008.

[12] Chang, C. C., Lee, G. W. and Yang, Y. G., “A New Indoor 3D Positioning Approach Using Single WiFi AP”, Journal of CCIT, Vol. 44, No. 2, pp. 1-10, 2015.

[13] Takasu, T., “RTKLIB Ver. 2.4.2 Manual”, http://www.rtklib.com/prog/manual_2.4.2.pdf, 2013.

[14] NovAtel Inc., “GPS Position Accuracy Measures”, APN-029 Rev 1, https://www.novatel.com/assets/Documents/Bulletins/apn029.pdf, 2003.